



Letter

Sintering and laser behavior of composite YAG/Nd:YAG/YAG transparent ceramics

Wenbin Liu^{a,b}, Yanping Zeng^b, Jiang Li^b, Yu Shen^c, Yong Bo^c, Nan Zong^c, Pengyuan Wang^c, Yiding Xu^c, Jialin Xu^c, Dafu Cui^c, Qinjun Peng^c, Zuyan Xu^c, Di Zhang^a, Yubai Pan^{b,*}^a State Key Laboratory of Metal Matrix Composites, Shanghai Jiao Tong University, Shanghai 200240, China^b State Key Laboratory of Transparent Opto-functional Inorganic Materials, Shanghai Institute of Ceramics, Chinese Academy of Sciences, Shanghai 200050, China^c Key Lab of Functional Crystal and Laser Technology, Technical Institute of Physics and Chemistry, Chinese Academy of Sciences, Beijing 100190, China

ARTICLE INFO

Article history:

Received 27 December 2011

Received in revised form 20 February 2012

Accepted 24 February 2012

Available online xxx

Keywords:

Sintering

Microstructure

YAG

Transparent ceramics

Optical properties

ABSTRACT

Highly transparent composite YAG/1.0 at.% Nd:YAG/YAG ceramic slab was prepared by vacuum reactive sintering method using commercial Al₂O₃, Y₂O₃ and Nd₂O₃ powders as raw materials with tetraethyl orthosilicate (TEOS) and La₂O₃ as sintering aids. By selecting the sintering aids and controlling their doping amounts, pure YAG and 1.0 at.% Nd:YAG ceramics can be well fabricated at the same sintering temperature. A fully dense composite ceramic slab with an average grain size of ~10 μm was obtained by sintering at 1750 °C for 50 h. The in-line transmittance of the composite ceramic was >81% near the visible wavelength of 400 nm. Output power of a composite ceramic rod (Ø3 mm × 82 mm) was 20.3 W with a pump power of 201 W, corresponding to an optical-to-optical conversion efficiency of 10.1%.

© 2012 Elsevier B.V. All rights reserved.

1. Introduction

Neodymium-doped yttrium aluminum garnet (Nd:YAG) single crystals have been widely used as a solid-state laser material in the various fields [1,2]. However, there remains the challenge of finding an approach that can overcome the technologic and economic issues of conventional single crystal laser gain media [3]. Since A. Ikesue, et al. firstly fabricated the Nd:YAG ceramics with highly efficient laser oscillation [4], Nd:YAG ceramics are considered to be a promising candidate because of its numerous advantages over single crystals, such as excellent laser performance, low cost, short preparation period, large size, high doping concentration and composite structure [5–7].

A significant problem with laser gain media, whether ceramics or single crystal, is thermal management. The active elements (e.g. Yb³⁺, Nd³⁺) doped into YAG can sharply degrade its thermal properties. For example, the thermal conductivity (~10 W/m K) of 1.0 at.% Nd:YAG is about 1.4 times lower than that of pure YAG [7]. In order to address this problem, the composite structure of YAG ceramic and single crystal was fabricated by vacuum sintering techniques

and thermal diffusion bonding, respectively [8,9]. The thermal concentration of local regions can be suppressed using composite structure design thanks to gradient distribution of active elements [3,10]. Unlike the complicated and expensive thermal diffusion bonding techniques [11], the fabrication of composite ceramics is a simple process which does not need high-precision optical polishing and thermal diffusion bonding. In the composite ceramics, the uniform microstructure can be observed, and the interface effect cannot be found between pure YAG and Nd:YAG regions. H. Yagi et al. reported the fracture strength of the composite Nd:YAG ceramic was the same as that of the noncomposite ceramic, the destruction point was not in interface region [12]. For composite Nd:YAG single crystals, the strength of the bonding interface is the lowest inside materials due to presence of residual thermal stress.

The purpose of this paper is to study solid-state reactive sintering of the composite ceramics and to make the preparation process for the composite ceramics as simple as possible. Microstructures and optical properties of the samples were investigated.

2. Experimental

2.1. Nd:YAG ceramics preparation

High-purity powders of α-Al₂O₃ (>99.99%, Alfa Aesar Company, USA), Y₂O₃ (>99.99%, Alfa Aesar Company, USA) and Nd₂O₃ (>99.99%, Alfa Aesar Company, USA) were used as starting materials. The powders were weighted precisely according to the chemical stoichiometry composition, with Nd³⁺ doping concentrations of 0 at.% and 1.0 at.%, respectively, and mixed by ball milling with high-purity Al₂O₃ balls

* Corresponding author at: Shanghai Institute of Ceramics, Chinese Academy of Sciences, 1295 Ding-Xi Road, Shanghai 200050, PR China. Tel.: +86 21 52412820; fax: +86 21 52413903.

E-mail address: ybpan@mail.sic.ac.cn (Y. Pan).

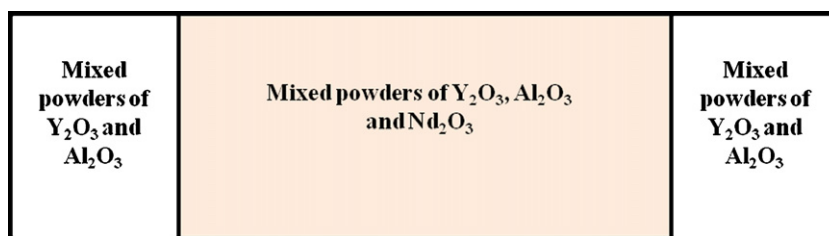


Fig. 1. Platform of the green body slab after pressing.

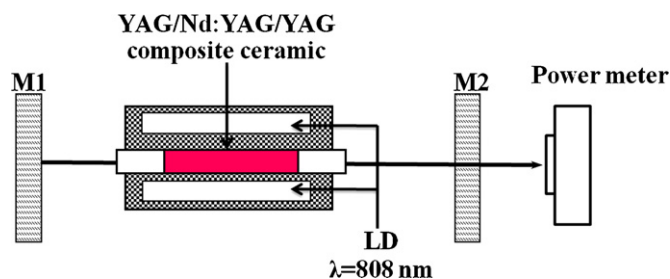


Fig. 2. Schematic diagram of experimental setup for diode-side pumped composite ceramic rod: M1, input mirror; M2, output mirror.

for 12 h in ethanol. Tetraethyl orthosilicate (TEOS, >99.99%, Alfa Aesar Company, USA) and La_2O_3 (>99.99%, Alfa Aesar Company, USA) were added as sintering aids. After ball milling, the slurries were dried at 70°C for 20 h in oven. The dry powders were sieved through a 200-mesh screen and calcined at 800°C for 4 h to remove the organic components. This general process is similar to that of the previous reports [13–17]. Using a custom designed steelless mould, the mixed powders were dry-pressed under 100 MPa and then cold isostatically pressed under 250 MPa. The platform of the green body slab after pressing is shown in Fig. 1. During the densification process, the powders formed pure YAG and 1.0 at.% Nd:YAG in situ as the oxide source powders react. The compacted pellets were sintered under vacuum of 10^{-5} Pa in the furnace equipped with tungsten mesh as heating element. After that, the samples were annealed in air at 1450°C for 20 h to completely remove internal stress and eliminate oxygen vacancies. After being mirror-polished on both surfaces, the composite YAG/1.0 at.% Nd:YAG/YAG transparent ceramic slab ($110\text{ mm} \times 55\text{ mm} \times 5\text{ mm}$) was obtained.

Microstructures of the polished and thermally etched surfaces of the samples were observed by electron probe microanalyzer (EPMA, Model JXA-8100, JEOL, Japan). The in-line transmittances were measured with spectrophotometer (Model Cary-5000, Varian, USA).

2.2. Laser experiment

The composite ceramic slab was processed into rod, which was 3 mm in diameter and consisted of a 54 mm long 1.0 at.% doped Nd^{3+} ions region and 14 mm long undoped end-caps. Experimental configuration of the composite ceramic rod is shown in Fig. 2. The laser system had one laser module in which a composite ceramic rod was used as laser medium. Both sides of the ceramic rod were antireflection coated at 1064 nm in order to reduce the intra-cavity losses. A maximum output power of 240 W LD with the emission wavelength of 808 nm was used as the pump source. The laser cavity adopted plano-plano symmetrical structure to get highly

efficient oscillation. M1 was coated with 99.8% high-reflectance at 1064 nm. M2 was the output coupler (OC) which was coated with 20% transmittance at 1064 nm.

3. Results and discussion

Fig. 3 (left) shows the mirror-polished composite ceramic with 0.8 wt% TEOS sintered at 1750°C for 50 h and annealed at 1450°C for 20 h. Words behind it can be seen clearly. The left region is pure YAG, and the right region is 1.0 at.% Nd:YAG. The in-line transmittances of the composite ceramic are shown in Fig. 3 (right). The transmittance of the Nd:YAG region is higher than that of the pure YAG region at the wavelength range of 200–1100 nm, which is very close to that of single crystal. However, for pure YAG region, the transmittances at 1064 nm and 400 nm are 76.5% and 73.9%, respectively. The drop-off in transmittance suggests the existence of optical scattering centers.

In order to investigate the main reason for decrease of the optical quality in pure YAG region, the microstructures of the composite ceramic vacuum-sintered were observed by EPMA (Fig. 4). The sample was sintered at 1750°C for 50 h, a full dense and pore-free microstructure is found in the Nd:YAG region with an average grain size of $\sim 10\ \mu\text{m}$ (Fig. 4(b)). For the pure YAG region, quite a few pores are remained inside the grains and between the grain boundaries (Fig. 4(a)). The average grain size is $\sim 5\ \mu\text{m}$, which is approximately twice smaller than that of Nd:YAG region. After sintering at 1765°C for 50 h, while all the other experimental conditions are the same, the grain size of the pure YAG region increases to $\sim 10\ \mu\text{m}$. The pores can be removed completely from the sample (Fig. 4(c)). As reported by W.D. Kingery [18], by B. Slamovich [19] and by S.-H. Lee [16], the grain growth is an important process to remove the final large pores. Higher sintering temperature helps to promote grain growth. However, abnormal grain growth is observed in the Nd:YAG region. Numerous pores and inclusions are found between or in the grains (Fig. 4(d)). Obviously, the addition of Nd_2O_3 results in lattice distortion of YAG by the substitution of Y^{3+} by Nd^{3+} . The formation of the energy of distortion causes an increase in the whole YAG system instability, and then decreases the sintering temperature of YAG. As a result, the sintering temperature of 1.0 at.% Nd:YAG

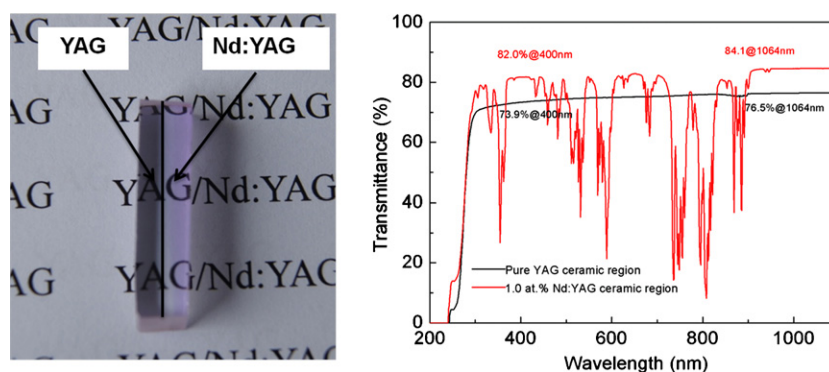


Fig. 3. Photo (left) and in-line transmittances (right) of the composite ceramic with 0.8 wt% TEOS sintered at 1750°C for 50 h.

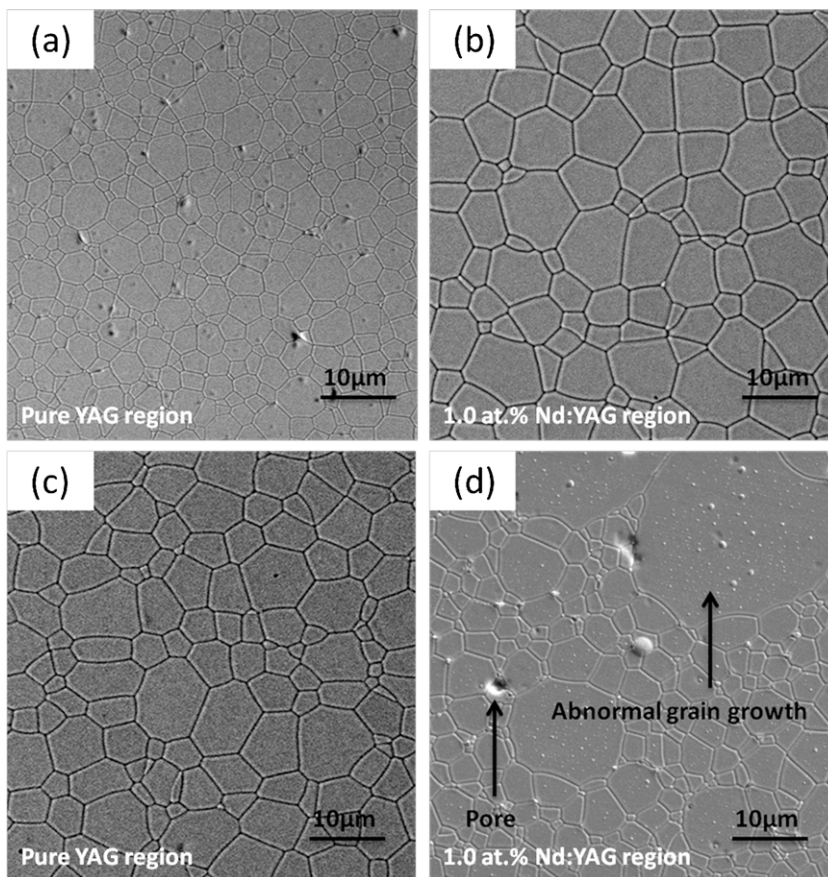


Fig. 4. EPMA micrographs of the thermal-etched surfaces of the composite ceramics sintered at 1750 °C (a, b) and 1765 °C for 50 h (c, d).

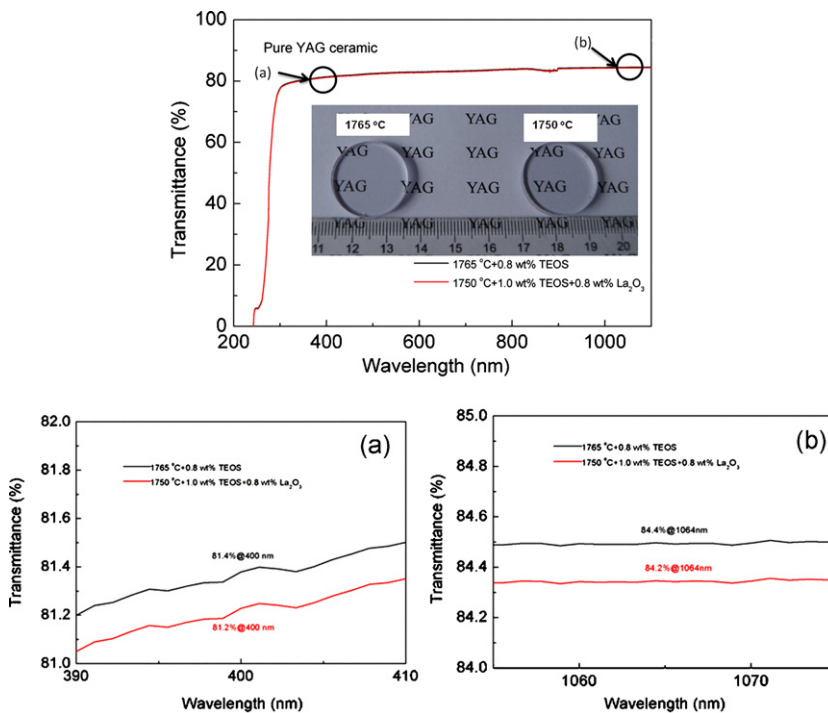


Fig. 5. In-line transmittances of the pure YAG ceramic with 1.0 wt% TEOS and 0.8 wt% La_2O_3 sintered at 1750 °C for 50 h and of pure YAG ceramic with 0.8 wt% TEOS sintered at 1765 °C for 50 h.

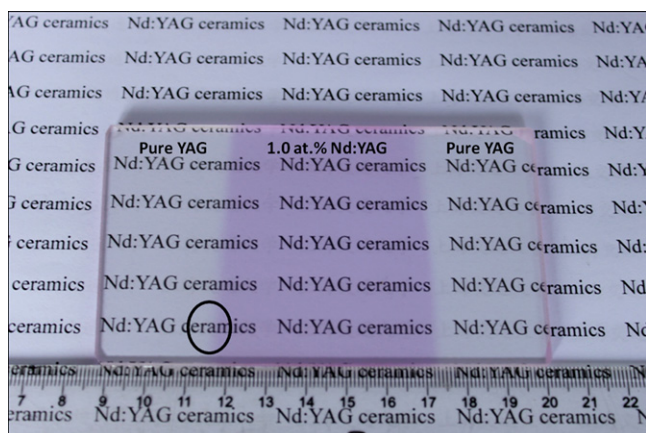


Fig. 6. Photo of the composite ceramic slab sintered at 1750 °C for 50 h, pure YAG region with 1.0 wt% TEOS and 0.8 wt% La₂O₃, Nd:YAG region with 0.8 wt% TEOS.

ceramic is a little lower than that of pure YAG ceramic. To fabricate highly transparent composite ceramic, it is necessary to find a way to decrease the sintering temperature of pure YAG ceramic without impairing optical quality.

According to previous works, the additions of TEOS and La₂O₃ are helpful to promote densification and decrease sintering temperature [15,20,21]. The transmittances of pure YAG ceramic with 1.0 wt% TEOS and 0.8 wt% La₂O₃ sintered at 1750 °C for 50 h are shown in Fig. 5. For comparison purpose, the pure YAG ceramic of the same size only with 0.8 wt% TEOS sintered at 1765 °C for 50 h was also prepared. In spite of the different sintering temperature, the transmittances of two ceramic samples are both >81% at the visible wavelength of 400 nm, and reach >84% with the wavelength shifting towards 1064 nm (Fig. 5). Overall, these results confirm that YAG ceramic with high optical quality can be obtained through adding multiple sintering aids and increasing their amounts, even at a lower sintering temperature.

As noted above, for the composite ceramic sintering, only 0.8 wt% TEOS was used as a sintering aid in the Nd:YAG region while the combination of 1.0 wt% TEOS and 0.8 wt% La₂O₃ were used in the pure YAG region. The photograph of the composite ceramic slab sintered at 1750 °C for 50 h and annealed at 1450 °C for 20 h is shown in Fig. 6. The whole sample is fully transparent, which is further demonstrated by the in-line transmittance spectrum, as shown in Fig. 7. The transmittance at the lasing wavelength of 1064 nm is 84.2% for pure YAG ceramic region and 84.3% for Nd:YAG ceramic region. The transmittances at 400 nm of pure YAG and Nd:YAG regions are 81.9% and 82.2%, respectively. The results prove that the

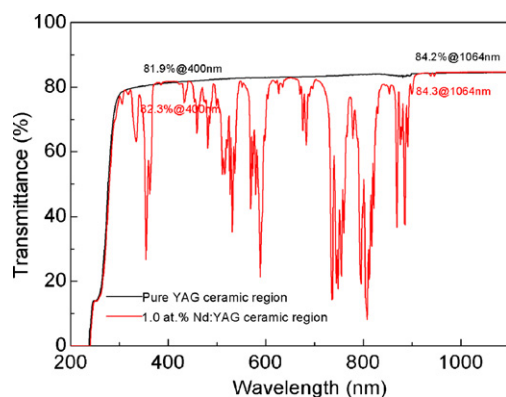


Fig. 7. In-line transmittances of the composite ceramic slab sintered at 1750 °C for 50 h, pure YAG region with 1.0 wt% TEOS and 0.8 wt% La₂O₃, Nd:YAG region with 0.8 wt% TEOS.

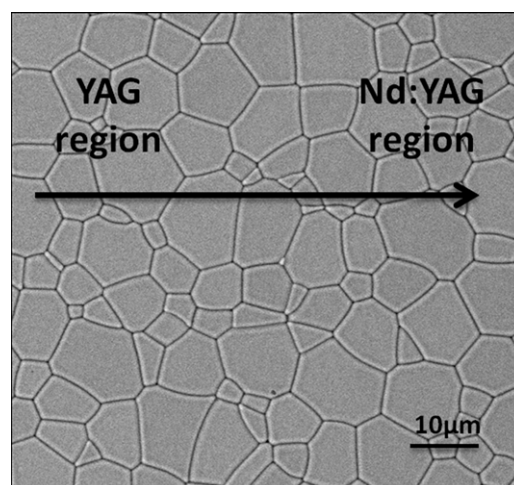


Fig. 8. EPMA micrograph of the composite ceramic slab sintered at 1750 °C for 50 h, pure YAG region with 1.0 wt% TEOS and 0.8 wt% La₂O₃, Nd:YAG region with 0.8 wt% TEOS.

in-line transmittances of the composite ceramic are nearly identical to the theoretical values of pure YAG and 1.0 at.% Nd:YAG single crystals grown by the Czochralski method [16].

Fig. 8 shows EPMA micrograph of the thermal-etched surface (marked region in Fig. 6) of composite ceramic. It is found that the sample exhibits a pore-free structure and the average grain size is ~10 μm. There are no trace of abnormal grain growth and no inclusions present both at the grain boundaries and in the grain matrix. From left (pure YAG region) to right (Nd:YAG region), the whole thermal-etched surface has a uniform microstructure, indicating that the interfacial effect does not appear in the composite ceramic.

Fig. 9 shows the thermal conductive values of pure YAG and 1.0 at.% Nd:YAG ceramics as a function of temperature. The thermal conductivity of pure YAG ceramic is 13.1 W/m K, which is 3.5 W/m K higher than that of 1.0 at.% Nd:YAG ceramic (9.6 W/m K) at room temperature. Furthermore, the thermal conductivities of pure YAG and 1.0 at.% Nd:YAG ceramics decrease with the increase of temperature, mainly due to the decrease of phonon mean free path. When the temperature is 600 °C, the corresponding thermal conductivities are 6.2 W/m K and 4.1 W/m K, respectively.

Output power of the 1064 nm composite ceramic laser rod versus incident pump power at 808 nm is shown in Fig. 10. It indicates that the laser output power is basically linear with the

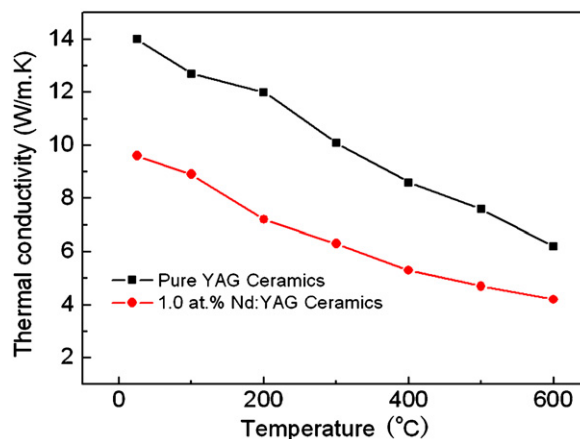


Fig. 9. The thermal conductivity values of pure YAG and 1.0 at.% Nd:YAG ceramics as a function of temperature.

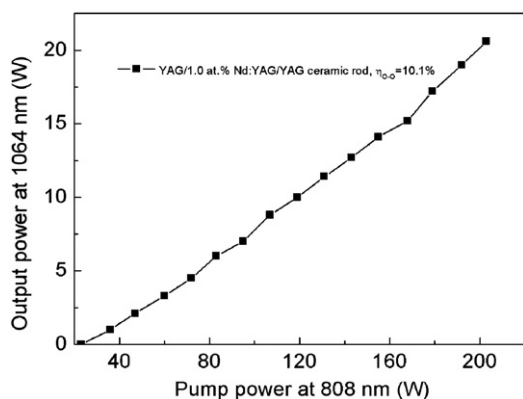


Fig. 10. Laser output power versus incident pump power.

incident pump power even at the highest power level. The threshold power is about 23 W. The output power is 20.3 W at a maximum pump power of 201 W, corresponding to an optical-to-optical conversion efficiency of 10.1%. It is worth noticing that there is no obvious evidence of saturation from the output power curve, suggesting that the higher output power will be obtained by further increasing the incident pump power. The result shows that the laser performance for ceramic is inferior to that for single crystal. This may attribute to the scattering loss mainly caused by a very small quantity of pores (cannot be detected by EPMA) in the ceramic [4,15]. Further work is in progress to optimize the fabrication techniques to further promote elimination of residual pores. We believe that higher output power of composite structure ceramic can be realized.

4. Conclusions

Transparent composite YAG/1.0 at.% Nd:YAG/YAG ceramic slab was successfully fabricated by solid-state reactive sintering method using high-purity commercial powders as raw materials and TEOS and La_2O_3 as the sintering aids. The sample sintered at 1750 °C for 50 h was fully dense with the average grain size of $\sim 10 \mu\text{m}$. No pores and other defects were found between or in the grains. The interface region between pure YAG and Nd:YAG showed a uniform microstructure, indicating that there was no interface effect present in the composite ceramic. The in-line transmittances of the sample at 1064 nm and 400 nm were $>84\%$ and $>81.5\%$, respectively, which was comparable to that of single crystal. Laser oscillation at

1064 nm was generated by diode-side-pumped composite ceramic rod. The threshold power was about 23 W. With the pump power of 201 W, the maximum output power of 20.3 W was obtained, corresponding to an optical-to-optical conversion efficiency of 10.1%.

Acknowledgments

The work was supported by Major Program of National Science Foundation of China (No. 50990300), the Key Program of Science and Technology Commission Foundation of Shanghai (No. 10JC1416000), the National High Technology Research and Development Program of China (No. 2010AA03015887003) and the National Natural Science Foundation of China (No. 51002172).

References

- [1] M.L. Saladino, G. Nasillo, D.C. Martino, E. Caponetti, J. Alloys Compd. 491 (2010) 737–741.
- [2] X.L. Zhang, D. Liu, Y.H. Sang, H. Liu, J.Y. Wang, J. Alloys Compd. 502 (2010) 206–210.
- [3] A. Ikesue, Ceramics laser materials, Nat. Photon. 2 (2008) 721–727.
- [4] A. Ikesue, T. Kinoshita, K. Kamata, K. Yoshida, J. Am. Ceram. Soc. 78 (1995) 1033–1040.
- [5] J. Li, W.B. Liu, B.X. Jiang, J. Zhou, W.X. Zhang, L. Wang, Y.Q. Shen, Y.B. Pan, J.K. Guo, J. Alloys Compd. 515 (2012) 49–56.
- [6] P. Samuel, T. Yanagitanic, H. Yagi, H. Nakao, K.I. Ueda, S.M. Babu, J. Alloys Compd. 507 (2010) 475–478.
- [7] J. Lu, K. Ueda, H. Yagi, T. Yanagitani, Y. Akiyama, A.A. Kaminskii, J. Alloys Compd. 341 (2002) 220–225.
- [8] J. Li, Y.S. Wu, Y.B. Pan, W.B. Liu, L.P. Huang, J.K. Guo, Int. J. Appl. Ceram. Technol. 5 (2008) 360–364.
- [9] E.C. Honea, R.J. Beach, S.C. Mitchel, J.A. Skidmore, M.A. Emanuel, S.B. Sutton, S.A. Payne, P.V. Avizonis, R.S. Monroe, D.G. Harris, Opt. Lett. 25 (2000) 805–807.
- [10] C. Bibeau, R.J. Beach, S.C. Mitche, M.A. Emanuel, J. Skidmore, C.A. Ebberts, S.B. Sutton, K.S. Ancaitis, IEEE J. Quant. Elect. 34 (1998) 2010–2019.
- [11] H.C. Lee, P.L. Brownlie, H.E. Meissner, E.C. Rea, SPIE 1624 (1991) 2–10.
- [12] H. Yagi, K. Takaichi, K. Ueda, Y. Yamasaki, T. Yanagitani, A.A. Kaminskii, Laser Phys. 15 (2005) 1338–1344.
- [13] T.D. Huang, B.X. Jiang, Y.S. Wu, J. Li, Y. Shi, W.B. Liu, Y.B. Pan, J.K. Guo, J. Alloys Compd. 478 (2009) L16–L20.
- [14] W.X. Zhang, J. Zhou, W.B. Liu, J. Li, L. Wang, B.X. Jiang, Y.B. Pan, X.J. Chen, J.Q. Xu, J. Alloys Compd. 506 (2010) 745–748.
- [15] W.B. Liu, J. Li, B.X. Jiang, D. Zhang, Y.B. Pan, J. Alloys Compd. 512 (2012) 1–4.
- [16] S.H. Lee, S. Kochawattana, G.L. Messing, J.Q. Dumm, G. Quarles, V. Castillo, J. Am. Ceram. Soc. 89 (2006) 1945–1950.
- [17] Y.K. Li, S.M. Zhou, H. Lin, X.R. Hou, W.J. Li, H. Teng, T.T. Jia, J. Alloys Compd. 502 (2010) 225–230.
- [18] W.D. Kingery, B. Francois, J. Am. Ceram. Soc. 48 (1965) 546–547.
- [19] E.B. Slamovich, F.F. Lange, J. Am. Ceram. Soc. 75 (1992) 2498–2508.
- [20] H. Yang, X.P. Qin, J. Zhang, S.W. Wang, J. Ma, L.X. Wang, Q.T. Zhang, J. Alloys Compd. 509 (2011) 5274–5279.
- [21] X.M. Hu, Q.H. Yang, C.G. Dou, J. Xu, H.X. Zhou, Opt. Mater. 30 (2008) 1583–1586.